Available online at www.sciencedirect.com

SCIENCE DIRECT®

Journal of Solid State Chemistry 177 (2004) 4073–4080

JOURNAL OF SOLID STATE CHEMISTRY

www.elsevier.com/locate/jssc

Hydrothermal synthesis and characterization of two new three-dimensional fluoroindium phosphates $In_4(PO_4)_4(H_2O)_4F_2 \cdot C_6H_{14}N_2$ and $In_8(PO_4)_8(H_2O)_8F_4 \cdot (C_5H_{14}N_2)_2$

Zhuo Yi, Yulin Yang, Keke Huang, Guanghua Li, Chao Chen, Wei Wang,
Yunling Liu, Wenqin Pang*

State Key Laboratory of Inorganic Synthesis and Preparative Chemistry, College of Chemistry, Jilin University,
Changchun 130012, People's Republic of China

Received 14 December 2003; received in revised form 10 June 2004; accepted 16 June 2004
Available online 7 October 2004

Abstract

Two new three-dimensional fluoroindium phosphates, $In_4(PO_4)_4(H_2O)_4F_2 \cdot C_6H_{14}N_2$ **1** and $In_8(PO_4)_8(H_2O)_8F_4 \cdot (C_5H_{14}N_2)_2$ **2**, have been prepared under hydrothermal conditions by using triethylenediamine and 1-methylpiperazine as templates, respectively. They are characterized by inductively coupled plasma analysis, elemental analysis, fluoride ion-selective electrode, IR spectra and thermogravimetric analysis. The structures have been solved by single-crystal X-ray diffraction. Both the compounds crystallize in the monoclinic system, space group $P2_1/n$ (No.14). Crystal data for **1**, $M = 1063.42$, $a = 10.3161(4)\,\text{Å}$, $b = 12.7490(3)\,\text{Å}$, $c = 17.9127(6)\,\text{Å}$, $\beta = 102.476(2)^\circ$, $V = 2300.25(13)\,\text{Å}^3$, $Z = 4$. Crystal data for **2**, $M = 2102.80$, $a = 18.4673(6)\,\text{Å}$, $b = 12.7117(5)\,\text{Å}$, $c = 20.4705(7)\,\text{Å}$, $\beta = 108.566(2)^\circ$, $V = 4555.4(3)\,\text{Å}^3$, $Z = 4$. They exhibit the same topological structure and are built up from vertex linking $InO_4(H_2O)_2$, InO_4FH_2O and InO_4F_2 octahedral and PO_4 tetrahedral units, forming 6-membered ring channels along the *a* direction and two types of 8-membered ring channels along the *b* direction. The diprontonated triethylenediamine and 1-methylpiperazine molecules are entrapped in 8-membered ring channels.

Keywords: Hydrothermal synthesis; Characterization; Triethylenediamine; 1-Methylpiperazine; Fluoroindium phosphates

1. Introduction

Research activities in the area of microporous metal phosphates have aroused wide interest due to their potential applications and rich architecture chemistry [1,2]. The majority of open-framework compounds have been synthesized hydrothermally or solvothermally by using diverse amines as templates. It is noted that one template can give rise to many different structures and that different templates can direct the formation of the same structure [3]. In group 13, with the increase of ionic radius of M^{3+} (Al, Ga and In), the tendency to form MPO_4 microporous compounds decreases [12]. Much attention has been paid to the lighter elements aluminum and gallium, and a large number of AlPOs and GaPOs with novel structures have been obtained [4–8]. During the past ten years, only fewer indium phosphates with various structural and compositional diversities have been synthesized in both hydrothermal and solvothermal systems by using the organic amines as templates. To our knowledge, there are three-dimensional (3-D) open-framework InPOs with In/P ratios of 1/2 [9], 2/3 [10,11], 1/1 [12], 9/8 [13], 5/4 [14], 6.8/5 [15],

---

*Corresponding author. Department of Chemistry, State Key Laboratory of Inorganic Synthesis and Preparative Chemistry, Jilin University, Changchun City, Jilin Province 130023, People's Republic of China. Fax: +86-431-5168624

E-mail address: wqpang@mail.jlu.edu.cn (W. Pang).

0022-4596/$ - see front matter © 2004 Elsevier Inc. All rights reserved.
doi:10.1016/j.jssc.2004.06.049

and (2-D) layers with In/P ratios of 1/3 [16], 1/2 [17,18], 4/7 [19], 1/1 [14]. Our scientific research group has reported on the synthesis of indium phosphates with different structures under hydrothermal and solvothermal conditions [14,28].

Fluoride method has proved to be an effective and promising method in promoting synthesis of large zeolite single crystals, novel metal phosphates and aluminosilicates [20–24]. Guth has summarized the role of F^- in the synthesis of microporous compounds [25]. By introducing fluoride into the synthetic system of metal phosphates, F^- acting as a mineralizer may enter the inorganic framework and favor the formation of novel compounds.

In this paper, we describe the hydrothermal synthesis and structural characterization of two new fluoroindium phosphates, $In_4(PO_4)_4(H_2O)_4F_2 \cdot C_6H_{14}N_2$ **1** and $In_8(PO_4)_8(H_2O)_8F_4 \cdot (C_5H_{14}N_2)_2$ **2**, by using triethylenediamine and 1-methylpiperazine as template in a fluoride-containing system.

2. Experimental

2.1. Synthesis and characterization

The two title compounds were synthesized hydrothermally from an aqueous mixture of indium nitrate (Shanghai Reagent Plant, 99.5%), phosphoric acid (Beijing Chemical Plant, 85%), triethylenediamine (Shanghai Chemical Reagent Company, 96%) (for compound **1**), 1-methylpiperazine (ACROS, 99%) (for compound **2**), hydrofluoric acid (Beijing Chemical Plant, 40%), and distilled water. Compound **1** was obtained from the gel composition 1.0 $In(NO)_3$: 2.0 H_3PO_4: 2.0 triethylenediamine: 5.0 HF: 250 H_2O, which was heated at 180 °C for 10 days in a Teflon-lined stainless-steel autoclave under autogeneous pressure. Compound **2** was prepared in a manner similar to **1** described above. The batch composition of 1.0 $In(NO)_3$: 2.0 H_3PO_4: 3.0 1-methylpiperazine: 6.0 HF: 460 H_2O was crystallized at 180 °C for 12 days. The resulting crystalline products consisting of colorless single crystals were filtered off, washed thoroughly with distilled water and dried overnight at room temperature.

The elemental analysis was performed on a Perkin-Elmer 2400 element analyzer and the inductively coupled plasma (ICP) was conducted on a Perkin-Elmer optima 3300 DV ICP spectrometer. F^- content was determined using a fluoride ion-selective electrode. The IR spectra were recorded on a Nicolet Impact 410 FTIR spectrometer within the 400–4000 cm^{-1} using KBr pellets. A NETISCH STA 449C unit was used to carry out the TGA analysis with a heating rate of 10 °C min^{-1} in air.

2.2. Determination of crystal structure

A suitable single crystal for each compound was selected and mounted on a glass fiber by using cyanoacrylate. The intensity data and structural analysis were collected on a Bruker Smart CCD diffractometer equipped with graphite-monochromated Mo$K\alpha$ radiation ($\lambda = 0.71073$ Å). The data processing was accomplished with the SAINT processing program [26]. The structure was solved by direct methods and refined by full-matrix least squares on F^2 using SHELXTL version 5.1 [27]. The indium and phosphorous atoms were first located and the carbon, nitrogen, fluorine, oxygen were founded in the final difference Fourier map. The hydrogen atoms of the amine molecule were located geometrically. CCDC reference numbers: 226403 and 226404. The data collection and refinement of compound **1** and **2** are shown in Table 1.

3. Results and discussion

3.1. Characterization

The ICP and elemental analysis are in good agreement with the values based on the single-crystal structure analysis. Calcd. for **1**: In, 43.19 wt%; P, 11.65 wt%; F, 3.57 wt%; C, 6.77 wt%; H, 2.07 wt%; N, 2.63 wt%. Found: In, 42.92 wt%; P, 11.47 wt%; F, 3.42 wt%; C, 6.70 wt%; H, 1.92 wt%; N, 2.55 wt%. Calcd. for **2**: In, 43.68 wt%; P, 11.78 wt%; F, 3.61 wt%; C, 5.61 wt%; H, 2.09 wt%; N, 2.66 wt%. Found: In, 43.52 wt%; P, 11.66 wt%; F, 3.40 wt%; C, 5.64 wt%; H, 2.31 wt%; N, 2.75 wt%. The TGA curve of compound **1** shows a total weight loss of 21.00% in the range of 200 and 900 °C (expected, 21.06%). The initial weight loss between 200 and 420 °C corresponds to the decomposition of the organic amine molecules (observed, 10.30%; expected, 10.72%). The second step occurring between 420 and 800 °C is assigned to loss of the structural H_2O molecules (observed, 7.00%; expected, 6.77%). The last weight loss of 3.70% between 800 °C and 900 °C corresponds to removal of F^- (expected, 3.57%). The TGA curve of compound **2** shows that major sections from 210 to 400, 400 to 720, and 720 to 900 °C are consistent with loss of organic amine (observed, 10.10%; expected, 9.70%), structural H_2O (observed, 7.15%; expected, 6.85%), fluoride ions (observed, 3.85%; expected, 3.61%), respectively. The IR spectrum of the compound **1** is assigned as follows: the strong and broad bands in 3500–3000 cm^{-1} region are typically attributed to O–H and N–H bands. The bands at 1614, 1470, 1157 cm^{-1} are assigned to δ_{O-H}, ν_{C-C}, ν_{C-N}, respectively. The bands at 1069, 1036 cm^{-1} are associated with asymmetric stretching vibrations of PO_4 unit. The bands at 589 and 543 cm^{-1} are related to bending vibrations of

Table 1
Crystal data and structure refinement for **1** and **2**

Empirical formula	$In_4(PO_4)_4(H_2O)_4F_2 \cdot C_6H_{14}N_2$	$In_8(PO_4)_8(H_2O)_8F_4 \cdot (C_5H_{14}N_2)_2$
Formula weight	1063.42	2102.80
Temperature 293(2) K	293(2) K	
Wavelength	0.71073 Å	
Crystal system	Monoclinic	Monoclinic
Space group	$P2_1/n$	$P2_1/n$
Unit cell dimensions (Å and °)	$a = 10.3161(4)$ $b = 12.7490(3)$ $c = 17.9127(6)$ $\beta = 102.476(2)$	$a = 18.4673(6)$ $b = 12.7117(5)$ c= 20.4705(7) $\beta = 108.566(2)$
Volume (Å^3)	2300.25(13)	4555.4(3)
Z	4	4
Density (calculated) (Mg/m^3)	3.071	3.092
Absorption coefficient (mm^{-1})	4.353	4.420
F (000)	2024	3944
Crystal size (mm)	$0.16 \times 0.04 \times 0.04$	$0.25 \times 0.05 \times 0.05$
θ range for data collection	1.98° to 24.97°	1.80° to 23.27°
Limiting indices	$-12 \leqslant h \leqslant 11$ $-15 \leqslant k \leqslant 15$ $-21 \leqslant l \leqslant 20$	$-20 \leqslant h \leqslant 20$ $-8 \leqslant k \leqslant 14$ $-22 \leqslant l \leqslant 22$
Reflections collected/unique	12419/4037 [R(int) = 0.0764]	21061/6501 [R(int) = 0.0604]
Completeness to $\theta = 23.25$	100.0%	99.4%
Refinement method	Full-matrix least-squares on F^2	
Data/restraints/parameters	4037/0/343	6501/0/667
Goodness-of-fit on F^2	1.035	1.004
Final R indices [$I > 2\sigma(I)$]^a	$R_1 = 0.0300$, w$R_2 = 0.0702$	$R_1 = 0.0326$, w$R_2 = 0.0806$
R indices (all data)	$R_1 = 0.0362$, w$R_2 = 0.0725$	$R_1 = 0.0504$, w$R_2 = 0.0897$
Largest diff. peak and hole	1.445 and −1.180 e Å^{-3}	1.257 and −1.039 e Å^{-3}

$^a R_1 = \sum||F_o| - |F_c|| / \sum|F_o| wR_2 = [\sum[w(F_o{}^2 - F_c{}^2)^2] / \sum[w(F_o{}^2)^2]]^{1/2}$.

In–O and PO_4 groups. The IR bands for compound **2**: $\nu_{N\text{–}H}$ and $\nu_{O\text{–}H}$, 3500–3000 cm^{-1}, $\delta_{O\text{–}H}$: 1641 cm^{-1}, $\nu_{C\text{–}C}$: 1470 cm^{-1}, $\nu_{P\text{–}O}$: 1068, 1039 cm^{-1}, $\delta_{In\text{–}O}$: 595 cm^{-1}, $\delta_{P\text{–}O}$: 542 cm^{-1}.

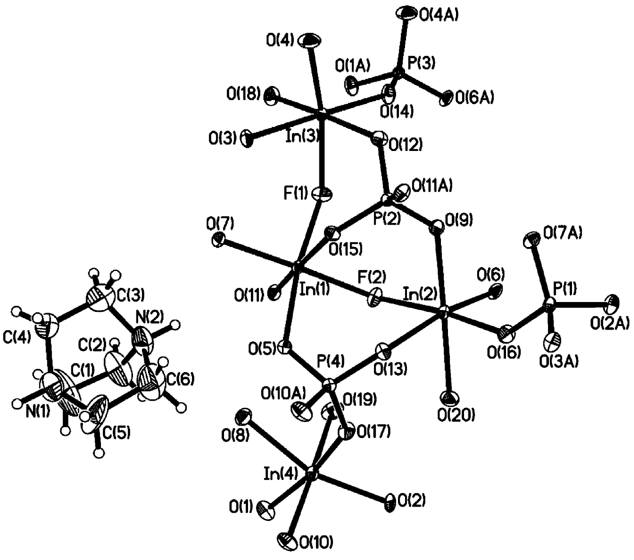

Fig. 1. ORTEP view of the structure of **1** showing the atom-labeling scheme (50% thermal ellipsoids).

3.2. Description of the structure

The atom-labeling scheme of **1** is shown in Fig. 1 and it contains four crystallographically distinct In atoms, four different P atoms and two F atoms. In(1) atom is octahedrally coordinated to four oxygen (In–O bond distances: 2.102(4)–2.120(4) Å) and two fluorine atoms (In–F bond distances: 2.118(3)–2.136(3) Å). In2 and In3 are both octahedrally coordinated to one fluorine (In–F bond distances: 2.122(3)–2.128(3) Å), one structural H_2O molecule (In–O bond distances: 2.215(4)−2.226(4) Å) and four bridging oxygen with adjacent P atoms (In–O bond distances: 2.077(4)–2.157(4) Å). In(4) is octahedrally coordinated to six oxygen atoms, of which four are bridging oxygen atoms with an In–O bond distances varying between 2.077(4) and 2.120(4) Å and the remaining two are structural H_2O molecules (In4–O8 and In4−O19 being 2.220(4) Å and 2.287(4) Å, respectively). The primary building unit $[InO_4(H_2O)_2]$ has a distorted octahedral configuration with the O–In–O bond angles falling in the range of 78.88(16)° to 170.54(16)°, which is attributed to the different coordination strengths of O^{2-} and H_2O ligands [12]. Of the four crystallographically distinct P atoms, each is coordinated to four oxygen atoms with adjacent indium atoms (P–O distances: 1.515(4)–1.564(4) Å). Both fluorine atoms are coordinated to adjacent indium atoms with bridging environments. The final atomic coordinates, and selected bond lengths are listed in Tables 2 and 3, respectively.

The atom-labeling scheme of **2** is shown in Fig. 2. The structure consists of eight crystallographically independent indiums, eight phosphorous and four fluorine atoms. In1 and In4 are octahedrally coordinated to four oxygen (In–O bond distances: 2.095(5)–2.135(4) Å) and two fluorine atoms (In–F bond distances: 2.127(4)–2.147(4) Å), While In2, In3, In5, and In6 are defined as InO_4FH_2O (In–F bond distances: 2.118(4)–2.134(4) Å, In–OH_2 bond distances: 2.188(5)–2.226(4) Å, In–O bond distances: 2.082(5)–2.145(5) Å) and the remaining In7 and In8 are as $InO_4(H_2O)_2$ (In–OH_2 bond distances: 2.250(5)–2.269(6) Å, In–O bond distances: 2.066(5)–2.121(5) Å). Of the eight phosphorous atoms, each shares four oxygen atoms with adjacent indium atoms (P–O bond distances: 1.518(5)–1.558(5) Å). All fluoride atoms act as bridging F^-. The final atomic coordinates, and selected bond lengths are listed in Tables 4 and 5, respectively.

Table 2
Atomic coordinates ($\times 10^4$) and equivalent isotropic displacement parameters ($Å^2 \times 10^3$) for **1**

Atom	*x*	*y*	*z*	*U* (eq)[a]
In(1)	7540(1)	5726(1)	2223(1)	9(1)
In(2)	10310(1)	3835(1)	2921(1)	10(1)
In(3)	5567(1)	5215(1)	3741(1)	10(1)
In(4)	11329(1)	6477(1)	778(1)	12(1)
P(1)	10652(1)	1162(1)	3076(1)	10(1)
P(2)	7204(1)	3402(1)	2992(1)	10(1)
P(3)	7026(1)	5896(1)	5584(1)	10(1)
P(4)	9191(1)	4538(1)	1079(1)	10(1)
F(1)	7127(3)	5939(3)	3322(2)	18(1)
F(2)	9518(3)	5377(2)	2822(2)	18(1)
O(1)	11737(4)	7950(3)	332(2)	19(1)
O(2)	13191(4)	5832(3)	1271(2)	15(1)
O(3)	4422(4)	5404(3)	2600(2)	15(1)
O(4)	3864(4)	4417(3)	3865(2)	23(1)
O(5)	8210(4)	5420(3)	1206(2)	14(1)
O(6)	11508(4)	4208(3)	4005(2)	16(1)
O(7)	5624(4)	6122(3)	1616(2)	14(1)
O(8)	9259(4)	7051(3)	636(2)	19(1)
O(9)	8676(4)	3407(3)	3393(2)	15(1)
O(10)	11389(4)	5984(3)	−319(2)	20(1)
O(11)	8254(4)	7290(3)	2301(2)	14(1)
O(12)	6355(4)	3711(3)	3575(2)	15(1)
O(13)	9392(4)	3717(3)	1723(2)	13(1)
O(14)	6740(4)	5203(3)	4868(2)	17(1)
O(15)	6924(4)	4158(3)	2313(2)	14(1)
O(16)	10923(4)	2277(3)	2814(2)	17(1)
O(17)	10549(4)	5037(3)	1077(2)	17(1)
O(18)	4988(4)	6838(3)	3967(2)	19(1)
O(19)	11418(4)	7269(4)	1933(3)	28(1)
O(20)	12010(4)	4310(3)	2415(2)	21(1)
N(1)	4898(7)	7476(6)	−1249(4)	45(2)
N(2)	5951(7)	7094(5)	99(4)	43(2)
C(1)	5697(13)	8434(8)	−878(6)	82(4)
C(2)	6349(10)	8157(7)	−109(5)	54(2)
C(3)	4464(9)	7110(8)	−7(5)	59(3)
C(4)	3865(8)	7304(8)	−821(5)	53(2)
C(5)	5778(10)	6637(10)	−1236(5)	74(4)
C(6)	6318(11)	6293(7)	−408(5)	64(3)

[a] *U* (eq) is defined as one-third of the trace of the orthogonalized U_{ij} tensor.

Table 3
Selected Bond Lengths (Å) for **1**

In(1)–O(7)	2.102(4)	In(4)–O(1)	2.118(4)
In(1)–O(15)	2.113(4)	In(4)–O(17)	2.120(4)
In(1)–F(1)	2.118(3)	In(4)–O(8)	2.220(4)
In(1)–O(5)	2.120(4)	In(4)–O(19)	2.287(4)
In(1)–O(11)	2.120(4)	P(1)–O(7)#1	1.533(4)
In(1)–F(2)	2.136(3)	P(1)–O(3)#1	1.539(4)
In(2)–O(16)	2.107(4)	P(1)–O(16)	1.541(4)
In(2)–O(9)	2.114(4)	P(1)–O(2)#2	1.538(4)
In(2)–O(6)	2.117(4)	P(2)–O(15)	1.530(4)
In(2)–F(2)	2.122(3)	P(2)–O(9)	1.533(4)
In(2)–O(13)	2.157(4)	P(2)–O(11)#1	1.549(4)
In(2)–O(20)	2.226(4)	P(2)–O(12)	1.552(4)
In(3)–O(4)	2.083(4)	P(3)–O(4)#3	1.539(4)
In(3)–O(14)	2.117(4)	P(3)–O(14)	1.534(4)
In(3)–F(1)	2.128(3)	P(3)–O(6)#4	1.539(4)
In(3)–O(12)	2.129(4)	P(3)–O(1)#5	1.549(4)
In(3)–O(3)	2.142(4)	P(4)–O(10)#6	1.515(4)
In(3)–O(18)	2.215(4)	P(4)–O(13)	1.538(4)
In(4)–O(10)	2.077(4)	P(4)–O(17)	1.539(4)
In(4)–O(2)	2.101(4)	P(4)–O(5)	1.564(4)

Symmetry transformations used to generate equivalent atoms: #1 $-x+3/2$, $y-1/2$, $-z+1/2$; #2 $-x+5/2$, $y-1/2$, $-z+1/2$; #3 $-x+1$, $-y+1$, $-z+1$; #4 $-x+2$, $-y+1$, $-z+1$; #5 $x-1/2$, $-y+3/2$, $z+1/2$; #6 $-x+2$, $-y+1$, $-z$.

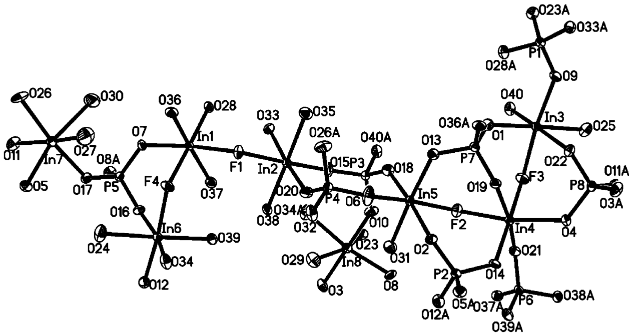

Fig. 2. ORTEP view of the structure of **2** showing the atom-labeling scheme (50% thermal ellipsoids).

Based on single-crystal X-ray diffraction analysis, compound **2** has the same inorganic topological framework structure as that of compound **1**. Compounds **1** and **2** do not have the same number of atoms in a unit cell, however they are isostructural to each other with different packing of building unit in space. Compound **1** is chosen as a model for structural description, which can be viewed as constructed from 2-D inorganic layers along the *a* direction: (i) $InO_4F(H_2O)$ octahedra and

Table 4
Atomic coordinates ($\times 10^4$) and equivalent isotropic displacement parameters ($\text{Å}^2 \times 10^3$) for **2**

Atom	x	y	z	U (eq)[a]
In(1)	2691(1)	9185(1)	136(1)	12(1)
In(2)	1245(1)	9791(1)	−1607(1)	12(1)
In(3)	−2147(1)	8877(1)	−6233(1)	12(1)
In(4)	−2842(1)	10796(1)	−5179(1)	12(1)
In(5)	−1295(1)	10238(1)	−3476(1)	12(1)
In(6)	2077(1)	11131(1)	1189(1)	13(1)
In(7)	4236(1)	8506(1)	2705(1)	16(1)
In(8)	709(1)	13532(1)	−2793(1)	16(1)
P(1)	−1965(1)	6206(2)	−6329(1)	13(1)
P(2)	−3084(1)	11227(2)	−3689(1)	12(1)
P(3)	570(1)	10905(2)	−3253(1)	12(1)
P(4)	−602(1)	9129(2)	−1847(1)	12(1)
P(5)	3898(1)	10406(2)	1483(1)	13(1)
P(6)	(1)	13452(2)	−5411(1)	13(1)
P(7)	−2122(1)	8442(2)	−4630(1)	13(1)
P(8)	−3971(1)	9573(2)	−6556(1)	13(1)
F(1)	1598(2)	9000(4)	−639(2)	18(1)
F(2)	−1716(2)	10974(4)	−4462(2)	19(1)
F(3)	−2236(2)	10426(4)	−5885(2)	21(1)
F(4)	2095(2)	9560(4)	838(2)	20(1)
O(1)	−1736(3)	8421(5)	−5193(2)	21(1)
O(2)	−2428(3)	10447(4)	−3427(2)	18(1)
O(3)	1026(3)	14938(5)	−2245(2)	22(1)
O(4)	−3859(3)	10456(4)	−6009(2)	18(1)
O(5)	3733(3)	9087(5)	3414(2)	20(1)
O(6)	−1147(3)	9458(5)	−2542(3)	30(2)
O(7)	3748(3)	9523(4)	932(2)	17(1)
O(8)	−340(3)	14077(4)	−3451(3)	20(1)
O(9)	−2235(3)	7315(4)	−6615(2)	19(1)
O(10)	316(3)	12068(4)	−3273(3)	26(1)
O(11)	5272(3)	9021(5)	3366(3)	23(1)
O(12)	2198(3)	12664(4)	1576(2)	22(1)
O(13)	−1513(3)	8729(4)	−3940(2)	19(1)
O(14)	−3408(3)	11211(4)	−4478(2)	16(1)
O(15)	1078(3)	10628(5)	−2532(3)	25(1)
O(16)	3264(3)	11237(4)	1278(2)	16(1)
O(17)	3912(3)	9934(5)	2175(2)	20(1)
O(18)	−151(3)	10220(5)	−3496(3)	22(1)
O(19)	−2775(3)	9245(4)	−4805(2)	16(1)
O(20)	110(3)	9818(5)	−1623(3)	21(1)
O(21)	−2698(3)	12360(4)	−5469(2)	16(1)
O(22)	−3333(3)	8748(4)	−6342(2)	18(1)
O(23)	1279(3)	14125(5)	−3455(3)	19(1)
O(24)	2565(3)	10582(6)	2265(3)	34(2)
O(25)	−2616(3)	9362(5)	−7310(3)	24(1)
O(26)	4650(3)	7020(5)	3126(3)	28(1)
O(27)	3109(4)	7717(6)	2171(3)	47(2)
O(28)	3296(3)	8782(4)	−541(2)	19(1)
O(29)	476(3)	12928(5)	−1845(3)	29(2)
O(30)	4441(4)	7927(5)	1733(3)	39(2)
O(31)	−1073(3)	11860(5)	−3091(3)	26(1)
O(32)	1838(3)	12758(6)	−2223(3)	37(2)
O(33)	2386(3)	9582(4)	−1629(2)	18(1)
O(34)	1001(3)	10801(5)	1301(2)	23(1)
O(35)	1054(3)	8180(5)	−2049(3)	25(1)
O(36)	2555(3)	7640(4)	464(2)	19(1)
O(37)	2601(3)	10753(4)	−238(2)	20(1)
O(38)	1377(3)	11285(4)	−1122(2)	18(1)
O(39)	1549(3)	11545(4)	138(2)	19(1)
O(40)	−1020(3)	9206(5)	−6236(2)	20(1)
N(1)	1133(5)	7414(7)	935(4)	49(2)
N(2)	−72(8)	7531(12)	−308(7)	112(5)
N(3)	3767(4)	2475(8)	−624(4)	50(2)
N(4)	5367(4)	2498(7)	179(4)	38(2)
C(1)	578(11)	8303(16)	791(9)	121(6)
C(2)	256(12)	8516(18)	93(10)	141(7)
C(3)	342(12)	6708(18)	−198(10)	134(7)
C(4)	713(10)	6450(15)	522(8)	109(6)
C(5)	1383(15)	7190(20)	1630(11)	195(11)
C(6)	4125(6)	1696(10)	−60(7)	65(4)
C(7)	4943(5)	1512(9)	38(6)	48(3)
C(8)	5048(6)	3294(9)	−366(6)	53(3)
C(9)	4224(6)	3479(10)	−451(6)	56(3)
C(10)	3643(7)	2118(13)	−1304(6)	75(4)

[a] U (eq) is defined as one-third of the trace of the orthogonalized U_{ij} tensor.

PO_4 tetrahedra share all of their corners with each other to form a kind of 8-MR (Fig. 3(a)), while InO_4F_2, $InO_4(H_2O)_2$ octahedra and PO_4 tetrahedra connect together giving rise to another kind of 8-MR (Fig. 3(b)). (ii) Two types of 8-MR are linked alternately, forming the 4, 6, 8-net 2-D inorganic layers along the *b* direction (Fig. 3(c)). It is different from $[C_5H_5NH]^+[In(HPO_4)(H_2PO_4)_2]$, which is constructed from ribbons of edge-sharing four-membered rings of alternating InO_6 and PO_4 units linked via $P(1)O_2(OH)_2$ groups forming the corrugated layer structure [16]. (iii) A series of this type of 2-D inorganic layers are further connected together via the In–O–P bonding to build the 3-D framework with 6-MR channels along the *a* direction (Fig. 4) and two types of eight 8-MR channels along the *b* direction (Fig. 5). The diprotonated triethylenediamine molecules that balance the charges of the framework are trapped in the main 8-MR channels, and they interact with the oxygens attached to the framework through H bonds. The N1–H1 group supplies one H to form H bond with the bridging O11 atom attached to P2 atom with the N1–O11 separation being 2.793 Å. The N2–H2 group tends to form two H bonds with bridging oxygen O7 attached to P1 and one oxygen O9 attached P2, the N2–O7 and N2–O9 distance being 3.071 Å and 3.130 Å, respectively. In contrast to the most reported indium phosphates with organic amines as structure directing agent, the compounds **1** and **2** exhibit the first 3-D open-framework with an In/P ratio of 1/1 and their structure contain two kinds of interconnected 8-MR. The framework of compound **2** is shown in Fig. 6 and the H-bonding for **1** and **2** are listed in Table 6. The results indicate that using different templates, triethylenediamine and 1-methylpiperazine, can direct the formation of fluoroindium phosphate with the same topological structures. The phenomenon can be seen in the synthesis of titanium phosphate [21]. It is likely that use of fluoride ions in the synthetic system of

Table 5
Selected bond lengths (Å) for **2**

In(1)–O(28)	2.100(5)	In(7)–O(27)	2.256(6)
In(1)–O(36)	2.116(5)	In(7)–O(30)	2.264(6)
In(1)–O(37)	2.122(6)	In(8)–O(8)	2.094(5)
In(1)–F(4)	2.125(4)	In(8)–O(3)	2.092(6)
In(1)–F(1)	2.146(4)	In(8)–O(23)	2.102(5)
In(1)–O(7)	2.151(5)	In(8)–O(10)	2.121(6)
In(2)–O(20)	2.087(5)	In(8)–O(29)	2.252(5)
In(2)–O(15)	2.107(5)	In(8)–O(32)	2.264(6)
In(2)–O(38)	2.121(5)	P(1)–O(28)♯1	1.529(5)
In(2)–F(1)	2.130(4)	P(1)–O(23)♯2	1.529(5)
In(2)–O(33)	2.137(5)	P(1)–O(33)♯1	1.533(5)
In(2)–O(35)	2.221(6)	P(1)–O(9)	1.547(6)
In(3)–O(1)	2.101(5)	P(2)–O(2)	1.525(5)
In(3)–F(3)	2.118(5)	P(2)–O(5)♯3	1.531(5)
In(3)–O(9)	2.121(5)	P(2)–O(14)	1.534(5)
In(3)–O(40)	2.126(5)	P(2)–O(12)♯4	1.541(6)
In(3)–O(22)	2.135(5)	P(3)–O(15)	1.516(5)
In(3)–O(25)	2.187(5)	P(3)–O(18)	1.535(6)
In(4)–O(14)	2.094(5)	P(3)–O(40)♯2	1.536(5)
In(4)–O(19)	2.104(5)	P(3)–O(10)	1.547(6)
In(4)–O(21)	2.116(5)	P(4)–O(6)	1.517(5)
In(4)–O(4)	2.138(5)	P(4)–O(20)	1.523(6)
In(4)–F(2)	2.141(4)	P(4)–O(34)♯3	1.526(5)
In(4)–F(3)	2.143(4)	P(4)–O(26)♯1	1.538(6)
In(5)–O(6)	2.093(5)	P(5)–O(8)♯5	1.520(5)
In(5)–O(13)	2.122(5)	P(5)–O(17)	1.532(5)
In(5)–O(18)	2.125(5)	P(5)–O(16)	1.533(5)
In(5)–F(2)	2.134(4)	P(5)–O(7)	1.552(5)
In(5)–O(2)	2.143(5)	P(6)–O(37)♯4	1.514(6)
In(5)–O(31)	2.199(6)	P(6)–O(39)♯4	1.539(5)
In(6)–O(12)	2.089(5)	P(6)–O(38)♯4	1.545(5)
In(6)–O(34)	2.114(5)	P(6)–O(21)	1.549(6)
In(6)–O(39)	2.124(5)	P(7)–O(19)	1.533(5)
In(6)–F(4)	2.125(4)	P(7)–O(36)♯1	1.536(6)
In(6)–O(16)	2.145(5)	P(7)–O(1)	1.536(5)
In(6)–O(24)	2.212(5)	P(7)–O(13)	1.543(5)
In(7)–O(11)	2.066(5)	P(8)–O(11)♯6	1.527(5)
In(7)–O(5)	2.091(5)	P(8)–O(22)	1.533(6)
In(7)–O(17)	2.101(5)	P(8)–O(3)♯4	1.540(5)
In(7)–O(26)	2.116(6)	P(8)–O(4)	1.552(5)

Symmetry transformations used to generate equivalent atoms: ♯1 $x-1/2, -y+3/2, z-1/2$; ♯2 $-x, -y+2, -z-1$; ♯3 $-x, -y+2, -z$; ♯4 $x-1/2, -y+5/2, z-1/2$; ♯5 $x+1/2, -y+5/2, z+1/2$; ♯6 $x-1, y, z-1$.

indium phosphates may result in novel framework structure with the unique ratio of In/P. $[In_{6.8}F_8(H_2O)_2(PO_4)_4(HPO_4)] \cdot 2H_2O \cdot [H_3N(CH_2)_2NH_2(CH_2)_2NH_3]_2 \cdot [H_2N(CH_2)_2NH_2(CH_2)_2NH_2]_2$ with a 3-D structure of extra-large 16-MR has been reported recently [15]. The fluorine atoms with both terminal and bridging environments allow the formation of the interesting tancoite chains. The tancoite chains are connected through a corner-shared chain forming a layer and are pillared by InO_4F_2 units. Another example with In_9P_8 composition is $[In_9(PO_4)_6(HPO_4)_2F_{16}] \cdot 3[H_2O] \cdot 4[H_3NCH_2CH_2NH_3] \cdot 3H_2O$, which is templated by 1,3-diaminopropane, and contains interconnected 8- and 14-MR channels through the framework [13]. The compound contains a rich chemistry with linear and bent fluoride bridges, terminal fluorides, and coordinated organic amine. In addition, two fluorinated indium phosphates, 3-D $[In_5P_4F_3O_{16}(H_2O)_2] \cdot$

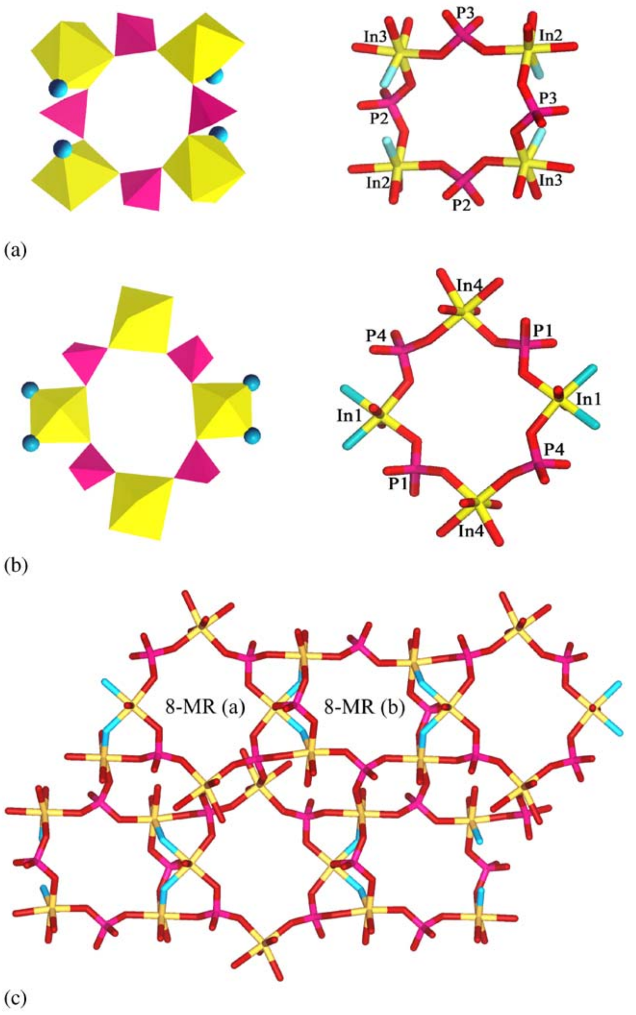

Fig. 3. Polyhedral and stick representation of 8-MR unit (a) and 8-MR unit (b). Small balls: F atoms. Stick representation of inorganic layer (c) along the [010] direction.

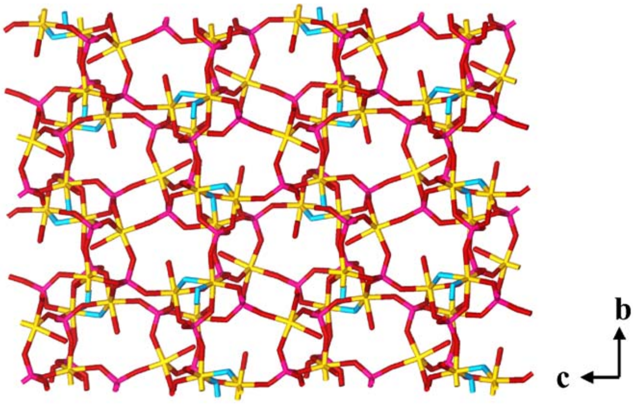

Fig. 4. Stick representation of **1** along the [100] direction, showing the 6-MR channels.

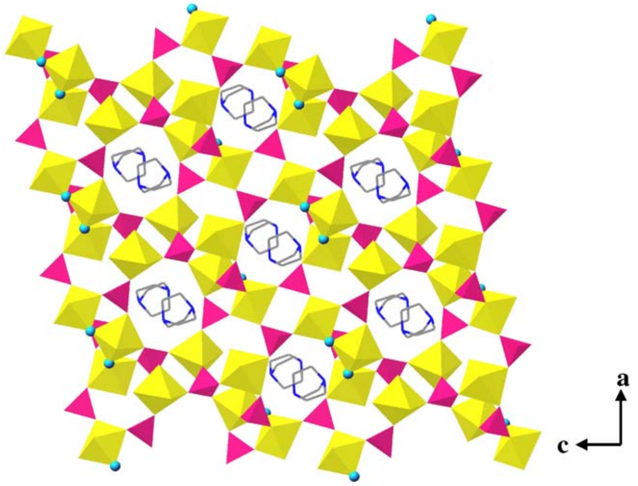

Fig. 5. Polyhedral view of **1** along the [010] direction, showing the 8-MR channels and the triethylenediamine molecules. Hydrogens on the amine molecule are not shown for clarity. Small balls: F atoms.

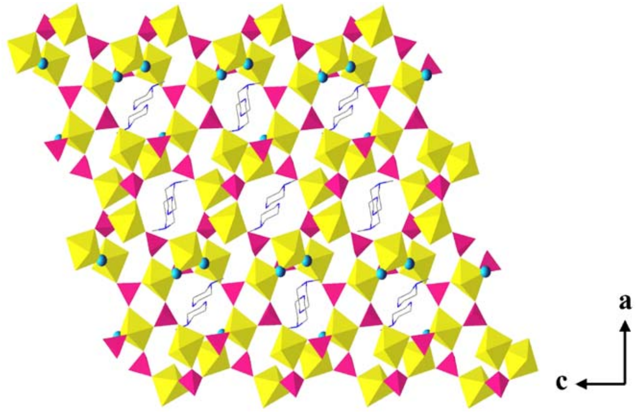

Fig. 6. Polyhedral view of the compound **2** along the [010] direction. Hydrogens on the amine molecule are not shown for clarity. Small balls: F atoms.

$[N_2C_2H_{10}]_3$ and 2-D $[InPO_4F]\cdot[H_2NCH_2CH_2NH_3]$ with ethylenediamine as the template have been reported [14].

4. Conclusions

Two new organically templated three-dimensional fluoroindium phosphates have been prepared hydrothermally by using triethylenediamine and 1-methylpiperazine as templates, respectively. Structural analysis indicates that both compounds have the same inorganic topological frameworks, which are constructed from strictly alternating $InO_4(H_2O)_2$, InO_4FH_2O and InO_4F_2 octahedra and PO_4 tetrahedra. There exist 8-MR channels along the *b* direction and 6-MR channels along the *a* direction in the framework structure and the diprotonated triethylenediamine and 1-methylpiperazine are trapped in the channels of 8-MR. The work indicates that the presence of HF and amines is crucial for the formation of open fluoroindium phosphates and the successful synthesis of 3-D fluoroindium phosphates will lead to new insights into the MPO_4 (Al, Ga and In) family. Further work on this theme is in progress.

Table 6
Hydrogen bonds for compounds **1** and **2** (Å and °)

D–H···A	*d* (H···A)	*d* (D···A)	Angle (D–H···A)
Compound **1**[a]			
N1–H1···O11♯1	1.914	2.793	161.90
N2–H2···O7	2.362	3.071	134.67
N2–H2···O9♯2	2.600	3.130	117.82
Compound **2**[b]			
N1–H1···O36	2.190	3.085	167.78
N2–H2C···O14♯1	2.406	3.179	144.04
N2–H2C···O39♯2	2.415	3.089	131.90
N2–H2D···O26♯3	2.240	3.134	171.69
N2–H2D···O34♯2	2.466	3.059	123.71
N3–H3···O21♯4	1.933	2.829	167.95
N4–H4A···O1♯5	2.110	2.779	130.45
N4–H4A···O28♯6	2.094	2.852	141.18
N4–H4B···O40♯5	2.374	3.032	130.01
N4–H4B···O10♯4	2.372	3.247	164.11

Symmetry transformations used to generate equivalent atoms:
[a] ♯1 $x-1/2, -y+3/2, z-1/2$; ♯2 $-x+3/2, y+1/2, -z+1/2$.
[b] ♯1 $-x-1/2, y-1/2, -z-1/2$; ♯2 $-x, -y+2, -z$; ♯3 $x-1/2, -y+3/2, z-1/2$; ♯4 $x+1/2, -y+3/2, z+1/2$; ♯5 $-x+1/2, y-1/2, -z-1/2$; ♯6 $-x+1, -y+1, -z$.

Acknowledgments

We are grateful for the financial support from the Ministry of Science and Technology of China through the State Basic Research Project (G200077507) and the National Natural Science Foundation of China (20233030).

References

[1] A.K. Cheetham, G. Férey, T. Loiseau, Angew. Chem. Int. Ed. 38 (1999) 3268–3292.
[2] S.H. Feng, R.R. Xu, Acc. Chem. Res. 34 (2001) 239–247.
[3] W.F. Yan, J.H. Yu, Z. Shi, R.R. Xu, Inorg. Chem. 40 (2001) 379–383.
[4] Q.S. Huo, R.R. Xu, S.G. Li, Z.G. Ma, J.M. Thomas, R.H. Jones, A.M. Chippindale, J. Chem. Soc., Chem. Commun. (1992) 875–876.
[5] M. Estermann, L.B. McCusker, C. Baerlocher, A. Merrouche, H.N. Kessler, Nature 352 (1991) 320–322.
[6] S. Girard, J.D. Gale, C. Mellot-Draznieksand, G. Férey, J. Am. Chem. Soc. 124 (2002) 1040–1051.
[7] Y.L. Yang, Y.L. Liu, Z.C. Mu, L. Ye, T. Hu, C. Chen, W.Q. Pang, J. Solid State Chem. 177 (2004) 696–700.
[8] C. Sassage, J. Marrot, T. Loiseau, G. Férey, Chem. Mater. 14 (2002) 1340–1347.

[9] S.S. Dhigra, R.C. Haushalter, J. Chem. Soc. Chem Commun. (1993) 1665–1666.

[10] S.S. Dhingra, R.C. Haushalter, J. Solid State Chem. 112 (1994) 96–99.

[11] Y.-F. Huang, K.-H. Lii, J. Chem. Soc. Dalton Trans. (1998) 4085–4086.

[12] Y. Xu, L.L. Koh, L.H. An, R.R. Xu, S.L. Qiu, J. Solid State Chem. 117 (1995) 373–378.

[13] I.D. Williams, J.H. Yu, H.B. Du, J.S. Chen, W.Q. Pang, Chem. Mater. 10 (1998) 773–776.

[14] H.B. Du, J.S. Chen, W.Q. Pang, J.H. Yu, I.D. Williams, Chem. Commun. (1997) 781–782.

[15] A. Thirumurugan, S. Natarajan, Dalton Trans. (2003) 3387–3391.

[16] A.M. Chippindale, S.J. Brech, Chem. Commun. (1996) 2781–2782.

[17] K.-H. Lii, Y.-F. Huang, Inorg. Chem. 38 (1999) 1348–1350.

[18] J.H. Yu, H.H.-Y. Sung, I.D. Williams, J. Solid State Chem. 142 (1999) 241–242.

[19] A.M. Chippindale, S.J. Brech, A.R. Cowley, W.M. Simpson, Chem. Mater. 8 (1996) 2259–2264.

[20] S. Qiu, J. Yu, G. Zhu, O. Terasaki, Y. Nozue, W. Pang, R. Xu, Micropor. Mesopor. 21 (1998) 245–251.

[21] Y.L. Fu, Y.L. Liu, Z. Shi, Y.C. Zou, W.Q. Pang, J. Solid State Chem. 162 (2001) 96–102.

[22] W.F. Yan, J.H. Yu, Z. Shi, Y. Wang, Y.C. Zou, R.R. Xu, J. Solid State Chem. 161 (2001) 259–265.

[23] Y.L. Liu, L.R. Zhang, Z. Shi, H.M. Yuan, W.Q. Pang, J. Solid State Chem. 158 (2001) 68–73.

[24] C.A. Fyfe, D.H. Brouwer, A.R. Lewis, L.A. Villaescusa, R.E. Morris, J. Am. Chem. Soc. 124 (2002) 7770–7778.

[25] J.L. Guth, K. Kessler, P. Caullet, J. Hazm, A. Merrouche, J. Patarin, In: R. von Ballmoos, J.B. Higgins, M.M.J. Treacy, (Eds.), Proceedings of the Ninth International Zeolite Conference, Butterworth-Heinemann, London, 1992, p. 215.

[26] SMART and SAINT (software packages), Siemens Analytical X-ray Instruments Inc., Madison, WI, 1996.

[27] SHELXTL, Version 5.1, Simens Industrial Automation, Inc., 1997.

[28] H.B. Du, J.S. Chen, W.Q. Pang, Progress in Zeolite and Microporous Materials Studies in Surface Science and Catalysis 105 (1997) 397–404.